Università degli Studi di Firenze

XUVLab

Dipartimento di Astronomia e Scienza dello Spazio

Preliminary results on the angular dependence of MAPMT response

Gianni Corti, Emanuele Pace, Marco Romoli

Dipartimento di Astronomia e Scienza dello Spazio, Università di Firenze, Firenze (Italy)

INFN Sezione di Firenze, Firenze (Italy)

Abstract

This paper reports on the preliminary results of the experiments on the angular dependence of a multi-anode photomultiplier tube (MAPMT) UV response. A 64-channel MAPMT produced by Hamamatsu K. K. has been irradiated at wavelengths in the range 250-400 nm and the output signal has been readout from a single pixel in photon counting mode. The final goal of this experimental activity, of which this measurements represent the first step, is to make an overall characterization of a micro-cell element (2×2 MAPMT), proposed as base element for assembling the EUSO focal surface. We discuss these preliminary results, taking into account the actual sources of experimental uncertainties, and we outline future setup upgrades and measurements needed to achieve the final micro-cell characterization including the light collector too.

Version 2.0

February 2002

Preliminary results on the angular dependence of MAPMT response

Gianni Corti, Emanuele Pace, Marco Romoli

Dipartimento di Astronomia e Scienza dello Spazio, Università di Firenze, Firenze (Italy)

INFN Sezione di Firenze, Firenze (Italy)

Abstract

This paper reports on the preliminary results of the experiments on the angular dependence of a multi-anode photomultiplier tube (MAPMT) UV response. A 64-channel MAPMT produced by Hamamatsu K. K. has been irradiated at wavelengths in the range 250-400 nm and the output signal has been readout from a single pixel in photon counting mode. The final goal of this experimental activity, of which this measurements represent the first step, is to make an overall characterization of a micro-cell element (2 × 2 MAPMT), proposed as base element for assembling the EUSO focal surface. We discuss these preliminary results, taking into account the actual sources of experimental uncertainties, and we outline future setup upgrades and measurements needed to achieve the final micro-cell characterization including the light collector too.

Introduction

The micro-cell is the base element of the EUSO focal surface assembly and it consists of a 2 × 2 array of MAPMT (Hamamatsu K.K., model R7600-03-M64), having 64 (8 × 8) 2-mm squared pixels each. The planned activity of the experimental group at the INFN/University of Florence laboratory mainly concerns the overall UV characterization of the micro-cells, that is the evaluation of their performances in terms of efficiency, linearity, uniformity, and cross-talk in the wavelength range of interest for the EUSO telescope (300-400 nm) [1]. Preliminarily, these tests will be limited to a single MAPMT, then to the micro-cell, and finally they will be performed to assess the performances of light collectors and MAPMT/micro-cell assembly.

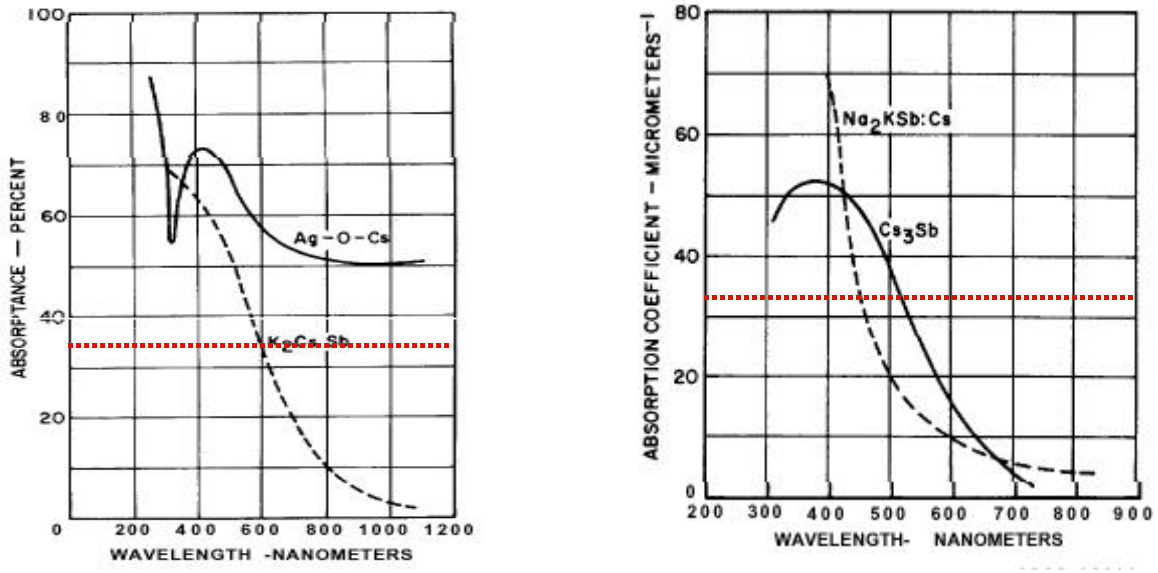

Figure 1. Spectral absorbance of some bialkali and trialkali photocathodes. The bialkali (K_2CsSb and Cs_3SB) are very similar to those used in the Hamamatsu 64-channel MAPMT. The red dotted line represents the inverse value of the typical photocathode thickness (graphs and data are from ref.2).

At this stage, we have started experimental tests on a MAPMT single pixel in order to study the angular dependence of the UV radiation response. The aim of this experiment is to assess possible efficiency losses due to the large incidence angles of the incoming UV radiation. The photon-electron conversion is obtained using a photocathode deposited on the internal side of the entrance window of a tube. The typical thickness of these photocathode layers is around a few tenths of nanometers, and this number must be compared with the mean absorption length of photons in the photocathodes. Fig. 1 shows the mean absorption length of some bialkali photocathodes [2] (the same used in the MAPMT) and the value of the typical thickness has been reported for comparison. It is possible to observe that not every incident photon with wavelength longer than 500-600 nm interacts with the photocathode and therefore some passes through. UV photons, instead, are always absorbed by the photocathode. This simple analysis makes evident that a different behavior can be expected when the incidence angle of the radiation on the photocathode is increased. Incident photons are absorbed and electrons are emitted isotropically over a 4π solid angle. Increasing the incidence angle, the photons are absorbed closer to the surface while the escape length for electrons increases. Therefore, it can be expected that at larger incidence angles the detector efficiency is higher than that derived from the 'cosine law' (efficiency decreasing due to geometrical variations of the exposed surface) for the visible photons, while it should be lower for the UV photons.
The results of tests performed on photomultipliers exposed to visible radiation confirm this hypothesis [3]. The tests we are going to discuss should give an answer to what is the behavior of MAPMT under UV irradiation increasing the incidence angle.

Angular dependence

The setup used for these tests is shown in Fig.2. A Low Pressure Mercury Lamp (Hamamatsu, mod. L1834) emits a photon flux, whose spectrum is reported in Fig.3. As the radiation has several components in the visible portion, an UG11 filter (Schott Glass Technologies Inc.), placed just in front of the lamp, transmits only the UV components falling below 400 nm (see the transmittance curve shown in Fig.4).
Thus, the UV radiation enters in an integrating sphere (Labsphere Inc.) through a 2 mm pinhole limiting the photon flux. The integrating sphere has a high internal reflectivity (about 90%) in the visible and much lower in the UV. Anyway, the advantage is that it provides a low-intensity isotropic radiation at the output. Coupling a long pipe to the sphere output, we should get a uniform and planar wave front. This pipe is internally blackened to prevent reflection on walls.

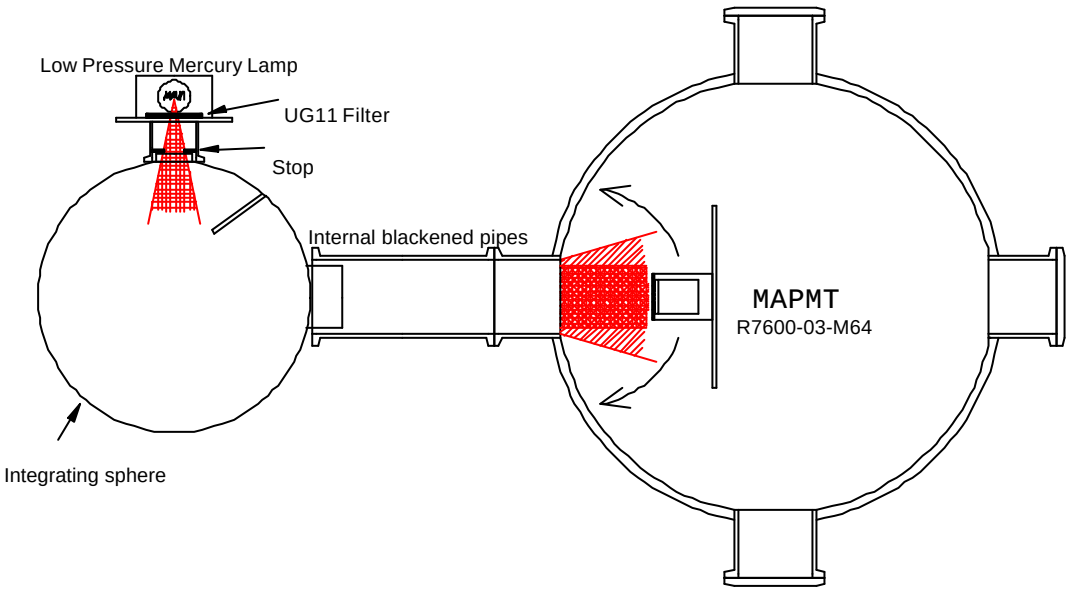

Figure 2. Sketch of the experimental setup for the preliminary tests on MAPMT.

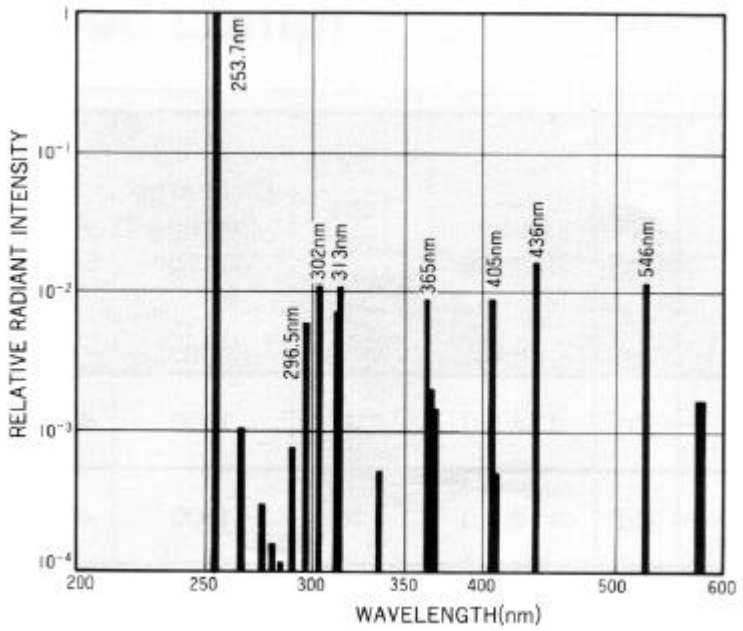

Figure 3. Hamamatsu L1834 Mercury lamp line spectra (see ref. 3).

Then, the radiation enters in a steel vacuum chamber that has been adapted to accommodate the MAPMT. Differently from what expected, the radiation emerging from the pipe is not perfectly uniform, but it presents an uniform circular region of the dimension of the integrating sphere exit flange (larger than the MAPMT size) plus a conic shadow having lower intensity that is due to the pipe vignetting.
The vacuum experimental chamber is operated in air for these tests. It has been used in order to have a visible-radiation free enclosure, as the chamber is completely sealed from the external environment. Next measurements will be done in vacuum to test the properties of MAPMT in an evacuated environment.

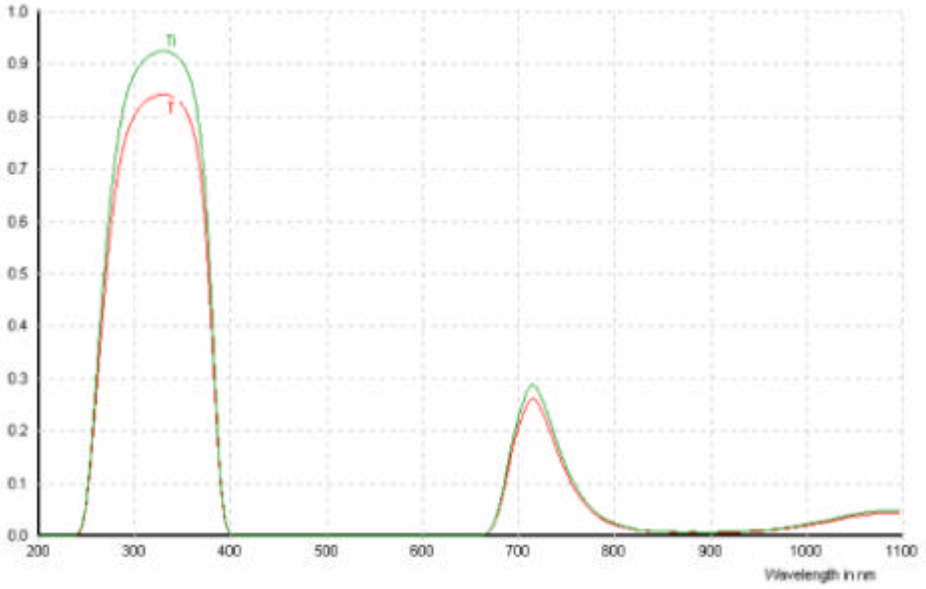

Figure 4. UG11 filter transmittance curve.

The MAPMT is mounted on a holder having the possibility to rotate with respect to the central vertical axis of the MAPMT entrance window to allow measurements of intensity with different incidence angle ranging from 0° to 60° with steps of 10°.
The MAPMT under test has an UV glass window and it is assembled with the standard voltage divider circuit and the case of the H7546 hybrid tube assembly.
The electronic board supporting the MAPMT allows the power supply connection and the signal readout by means of a coaxial cable that can be weld to a pin of the MAPMT socket, corresponding to a single pixel. The signal readout is performed in photon counting mode by means of a preamplifier, a discriminator and a digital counter. Some of the main parameter values of the instrumentation settings are reported in Table 1.

Table 1. Measurement parameters.

Source Power (VA)	11.4 V × 0.19 A
MAPMT High Voltage Supply	- 800 V
MAPMT single pixel current*	0.36 μA
Counter Gate Time	1 sec

* The MAPMT is fully illuminated and the 64 channels are all biased.

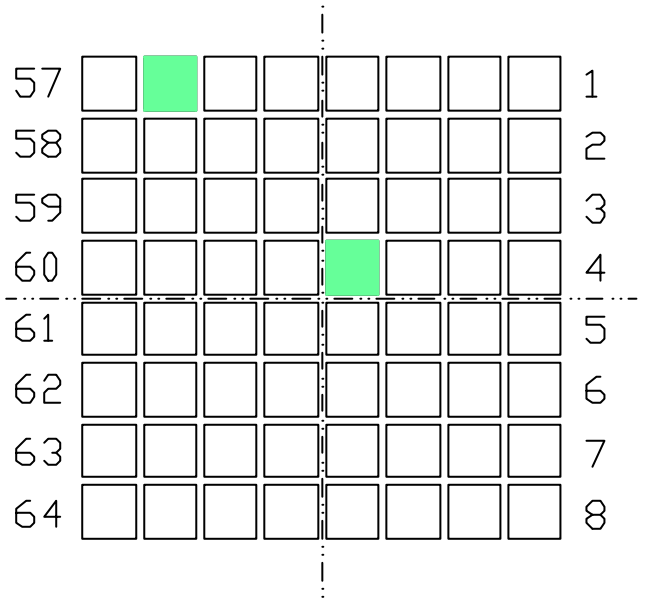

Figure 5. The MAPMT pixel map with the two tested pixels highlighted.

The MAPMT detected dark counts are less than 10 counts/sec. This number can be considered negligible if compared to a typical signal count rate (about 10^5 count/s).
The pixels that have been analyzed are two: one central pixel (P28) and one edge pixel (P49) (see Fig.5). The central pixel has been chosen with no specific reasons, while the edge pixel has been selected because of its sensitivity much lower than the others (data provided by the manufacturer on the pixel uniformity, see ref.4).

The resulting normalized UV response in function of the incidence angle is plotted in Figs.6 and 7 for the two different pixels. The two sets of data shown in Fig.7 refer to two different measurements separated by a long time period. This is in order to verify the repeatability of the measurement.

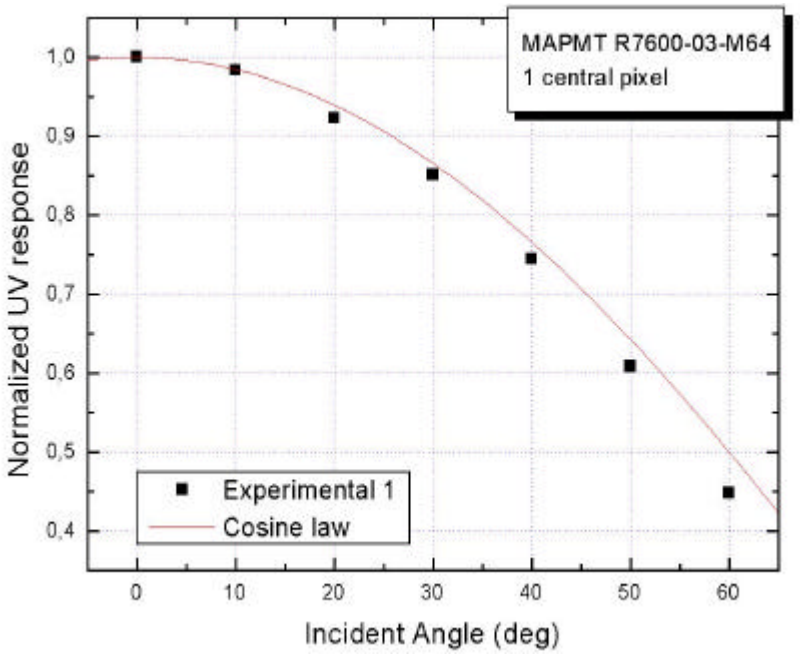

Figure 6. Angular dependence of the UV response for the central pixel (P28).

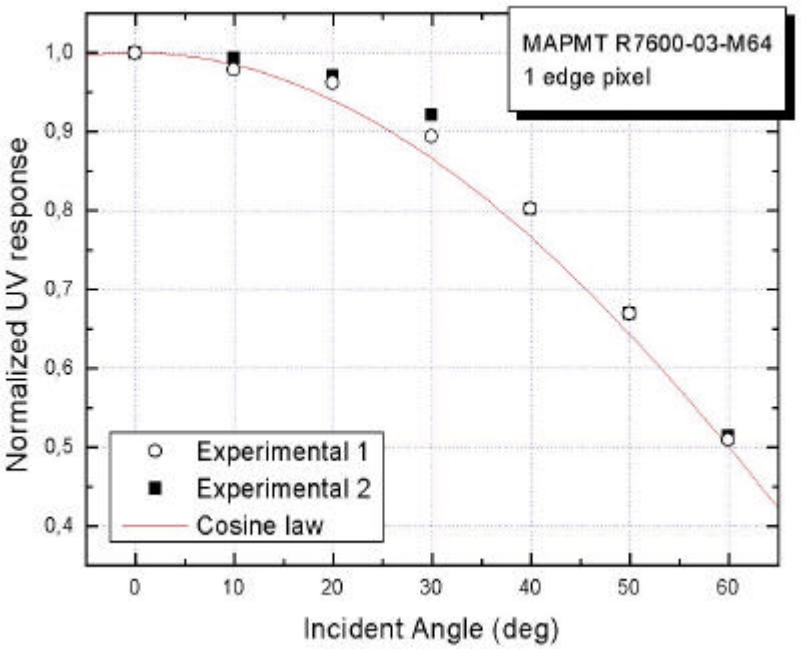

Figure 7. Angular dependence of the UV response for the edge pixel (P49).

As it is evident from the plots, the behavior of the photoresponse is very close to a cosine law as expected if only the geometrical effects, due to the MAPMT rotation, affect the measurements.

The discrepancies between the data and the cosine law may be due to different errors concerning the setup arrangement and the source stability. In particular, the rotational system is mechanical and it is not very accurate in the angle position and in the position of the rotational axis, then it is possible that this generates some systematic error. The beam of light illuminating the MAPMT window is supposed to be uniform and collimated, but this assumption is 'almost' correct: the light escaping the entrance aperture in the measurement chamber is uniform in the central part and not at the edges, but it is not very collimated. Furthermore the UG11 filter has not been tested to verify its transmission stability when exposed to high UV fluxes and to temperature gradient. Taking into account all these possible error sources, a small deviation

from the cosine law can be observed at angles greater than 30°. This is pointed out by the results from the central pixel. The same behavior can be observed also for the edge pixel if some aspects are considered. The MAPMT rotates around the central vertical axis of the entrance window. Therefore, the edge pixel is slightly closer to the radiation source after a MAPMT rotation and its position is as closer as greater is the incidence angle. This effect is partially compensated by a somewhat lower intensity due to a non-perfectly uniform radiation beam, but it can cause the observed better efficiency. Nevertheless, it can be also observed that at angles greater than 30° the difference between measured efficiency values and the cosine law decreases up to 60°, where there is no more difference. This global behavior could be interpreted as the combination of two effects: the systematic error due to the misalignment of the edge pixel with the rotational axis and the efficiency angular decrease observed after the central pixel measurement.
These results will be clarified after the next session of measurements, performed with a much better instrumentation arrangement.

Next improvements and measurements

With the present setup it is possible to make further testing of the angular dependence of other pixel responses; furthermore, it is possible to study the linearity versus gain and the efficiency of the single pixels in the UV, provided that a power meter or a calibrated photodiode is available.
Several future improvements of these preliminary measurements have been already planned. Firstly, a set of measurements with a pulsed Nitrogen laser (337.1 nm emission peak) with a near-diffraction limited beam (0.3 mrad) and a pulse width of 4 ns FWHM have been scheduled. These features of the laser allow measurements of very short pulses, that is of the MAPMT time response versus gain, of a precise angular dependence, of dead time or the detectable count rate of each pixel, as well as the mapping of uniformity under UV irradiation. It will be also possible to simulate the fluorescence light track due to an EAS (Extensive Air Showers) event by means of coupling the Nitrogen laser to appropriate stops and filters: this will be a rough test of the micro-cell performances in recovering an EAS event.
In addition, the detector mounting setup will be improved to eliminate the systematic errors. A motorized rotation-translation stage will substitute for the mechanical mounting in order to improve alignment of the tube with the radiation beam. Shortly, a new printed circuit board (PCB) to arrange the four MAPMTs of the micro-cell will be completed [5]. This will allow a better detector mounting and the parallel readout of the pixels via multi-channel ADC. This setup will permit also an accurate measurement of uniformity and cross talk.

References

[1] L. Scarsi, et al., “EUSO – Extreme Universe Space Observatory”, Proposal for the ESA F2/F3 Mission, January 2000.
[2] Photomultiplier Handbook, Burle Industries, Inc., USA (Dec. 89).
[3] Photomultiplier tube: principle to application, Hamamatsu Photonics K. K., Japan (1994).
[4] Multi-anode photomultiplier tube R5900/R7600, data sheet, Hamamatsu Photonics K. K.
[5] M. Ameri et al., Study report on the EUSO photo-detector design, INFN Techn. Rep., (2001).